

Research Article

Cite this article: Wu C, Goldsmith M-R, Pawlak J, Feng P, Smith S, Navarro S, Perez-Jones A (2020) Differences in efficacy, resistance mechanism and target protein interaction between two PPO inhibitors in Palmer amaranth (*Amaranthus palmeri*). *Weed Sci.* **68**: 105–115. doi: [10.1017/wsc.2020.4](https://doi.org/10.1017/wsc.2020.4)

Received: 4 November 2019
Revised: 23 December 2019
Accepted: 27 December 2019
First published online: 13 January 2020

Associate Editor:

Franck E. Dayan, Colorado State University


Keywords:

PPX2 mutations; protoporphyrinogen oxidase (PPO) inhibitors; target-site resistance

Author for correspondence:

Chenxi Wu, Bayer CropScience, 700 Chesterfield Parkway West, St Louis, MO 63017.
Email: chenxi.wu@bayer.com

Differences in efficacy, resistance mechanism and target protein interaction between two PPO inhibitors in Palmer amaranth (*Amaranthus palmeri*)

Chenxi Wu¹ , Michael-Rock Goldsmith¹, John Pawlak², Paul Feng¹, Stacie Smith¹, Santiago Navarro¹ and Alejandro Perez-Jones¹

¹Bayer CropScience, St Louis, MO, USA and ²Valent USA, Walnut Creek, CA, USA

Abstract

A weed survey was conducted on 134 Palmer amaranth (*Amaranthus palmeri* S. Watson) populations from Mississippi and Arkansas in 2017 to investigate the spread of resistance to protoporphyrinogen oxidase (PPO) inhibitors using fomesafen as a proxy. Fomesafen resistance was found in 42% of the *A. palmeri* populations. To investigate the resistance basis of different PPO inhibitors, we further characterized 10 representative populations by *in planta* bioassay in a controlled environment and molecular characterizations (DNA sequencing and TaqMan® gene expression assay). A total of 160 plants were sprayed with a labeled field rate (1X) of fomesafen or saflufenacil and screened for the presence of three known resistance-endowing mutations in the mitochondrial *PPX2* gene (Δ Gly-210, Arg-128-Gly, Gly-399-Ala). To compare the potencies of fomesafen and saflufenacil, dose-response studies were conducted on two highly resistant and one sensitive populations. The interaction of the two herbicides with the target protein harboring known *PPX2* mutations was also analyzed. Our results showed that: (1) 90% of the fomesafen- or saflufenacil-resistant plants have at least one of the three known *PPX2* mutations, with Δ Gly-210 being the most prevalent; (2) saflufenacil is more potent than fomesafen, with five to nine times lower resistance/susceptible (R/S) ratios; (3) fomesafen selects for more diverse mutations, and computational inhibitor/target modeling of fomesafen suggest a weaker binding affinity in addition to a smaller interaction volume and volume overlap with the substrate protoporphyrinogen IX than saflufenacil. As a result, saflufenacil shows reduced sensitivity to *PPX2* target-site mutations. Results from current study can help pave the way for designing weed management strategies to delay resistance development and maintain the efficacy of PPO inhibitors.

Introduction

Protoporphyrinogen oxidase (PPO) is the last common enzyme that oxidizes protoporphyrinogen IX (ProtoG) to protoporphyrin IX (ProtoX) in the tetrapyrrole pathway in higher plants (Beale and Weinstein 1990). The tetrapyrrole pathway produces important precursor molecules for the biosynthesis of chlorophyll and heme, which are needed for photosynthesis and electron transfer chains, respectively (Grimm 1998; Heinemann et al. 2008; von Wettstein et al. 1995). Inhibition of PPO by herbicides leads to the accumulation and leakage of the PPO substrates into the cytoplasm; the resulting reactive oxygen species disintegrate lipids and protein membranes, leading to plant death (Duke et al. 1991; Jacobs and Jacobs 1993; Lee and Duke 1994). First introduced to the market in the 1960s, PPO inhibitors now have been classified into four major chemistry families: (1) diphenylether (e.g., fomesafen, lactofen); (2) N-phenylphthalimide (e.g., flumioxazin); (3) aryl triazinone (e.g., sulfentrazone, carfentrazone); and (4) pyrimidinedione (e.g., saflufenacil). PPO inhibitors, applied both PRE and POST (Grossmann et al. 2010; Harder et al. 2012; Wuerffel et al. 2015b), mainly control broadleaf weeds, with some exceptions that are active on grasses (Larue et al. 2019; Selby et al. 2015).

The evolution and spread of weed resistance to this herbicide group was relatively slow. However, the use of PPO inhibitors increased dramatically due to the widespread occurrence of weeds resistant to glyphosate and acetolactate synthase (ALS) inhibitors (Dayan et al. 2017). Resistance to PPO inhibitor was first documented in 2001 in Kansas in a common waterhemp (*Amaranthus tuberculatus* var. *rudis*) biotype that was also resistant to ALS inhibitors (Heap 2019). So far, 10 broadleaf and 3 grass weed species have been reported to have evolved resistance to PPO inhibitors globally (Heap 2019). PPO-inhibitor resistance in key weed species such as *A. tuberculatus* var. *rudis* and Palmer amaranth (*Amaranthus palmeri* S. Watson), have been documented in eight and three U.S. states, respectively (Heap 2019; Salas-Perez et al. 2017; Varanasi et al. 2018b). More problematically, both weed species are well known for their dioecious nature, which enables pollen-mediated movement and facilitates rapid spread of

the resistance genes. As a result, *Amaranthus* spp. have a higher propensity for stacking multiple resistance traits, leaving farmers very limited control options (Evans et al. 2019; Shergill et al. 2018).

PPO enzyme isoforms are localized in two cellular compartments, one in the chloroplast (encoded by *PPX1*) and one in the mitochondria (encoded by *PPX2*) (Lermontova et al. 1997). *PPX2* sometimes can be dual-targeting, which might be an important attribute that facilitates the evolution of resistance (Watanabe et al. 2001). Although chloroplastic isoform *PPX1* is the primary target of PPO inhibitors, weeds appear to favor *PPX2* as their resistance evolutionary pathway (Dayan et al. 2017). The first elucidated resistance mechanism for PPO inhibitors was target-site resistance (TSR) via an unusual codon deletion at the 210 position (Δ Gly-210) in the *PPX2* gene in *A. tuberculatus* var. *rudis* (Patzoldt et al. 2006). Since then, other *PPX2* mutations have been found to confer PPO-inhibitor resistance in common ragweed (*Ambrosia artemisiifolia* L.) (Arg-98-Leu) and *A. palmeri* (Arg-98-Gly, Arg-98-Met, Gly-399-Ala) (Giacomini et al. 2017; Rangani et al. 2019; Rousonelos et al. 2012). Most recently, a resistance-endowing mutation was reported in goosegrass [*Eleusine indica* (L.) Gaertn.] (Bi et al. 2019). Furthermore, overexpression of *PPX2* enzyme, although not yet found in any weed species, was used to generate transgenic crops with PPO-inhibitor resistance and thus could be another potential resistance mechanism that could evolve in weeds (Choi et al. 1998; Lee et al. 2000; Watanabe et al. 2002). Even though target-site mutations are the primary resistance mechanism in many species, there are indeed some PPO resistant weeds that do not contain *PPX1* or *PPX2* mutations, indicating the possibility of non-target site based resistance mechanisms (NTSR) in these biotypes (Copeland et al. 2018; Varanasi et al. 2018a, 2019). Real-time knowledge on the spread and the genetic basis of herbicide resistance is critical to design effective resistance mitigation strategies that sustain the efficacy and durability of a limited set of currently effective herbicides, including PPO inhibitors. In this paper, we surveyed 134 *A. palmeri* populations from Mississippi and Arkansas for resistance to fomesafen, a commonly used PPO inhibitor. In addition, we characterized 10 representative populations to understand the genetic basis of resistance, focusing on the roles of three known *PPX2* mutations in conferring PPO-inhibitor resistance in *A. palmeri*. Efficacy and resistance basis for two commonly used PPO inhibitors, fomesafen and saflufenacil, were investigated through DNA sequencing, protein modeling, and *in planta* bioassay in the greenhouse. The goal of this investigation was to address the following key questions: (1) Do different PPO inhibitors select for different *PPX2* mutations? (2) Are *PPX2* mutations equally effective in conferring resistance against PPO inhibitors with different potencies? (3) Do different PPO inhibitors differ in their interactions with the wild-type or mutated target protein?

Materials and Methods

Survey of Fomesafen Resistance on 134 *Amaranthus palmeri* Populations

A total of 134 *A. palmeri* populations were collected from Mississippi and Arkansas states along the Mississippi River during 2016. Eight plants from each population were grown at the Bayer CropScience greenhouse facility at Chesterfield, MO, under standard conditions (14-h photoperiod, 29 C day/ 26 C night, 30% to 85% relative humidity). Plants at 10 to 15 cm in height were sprayed with fomesafen (Flexstar® herbicide, Syngenta Crop Protection, P.O.Box 18300, Greensboro, NC 27419, USA) at

Table 1. Location and GPS coordinates for the 10 *Amaranthus palmeri* populations selected for further greenhouse and molecular characterization.

Population ID	Location	Latitude °N	Longitude °W	Response to fomesafen ^a
P1	Durhamville, TN	35.6328	89.4663	R
P2	Durhamville, TN	35.6328	89.4663	R
P3	Sharkey County, MS	32.9250	90.8992	S
P4	Desoto County, MS	34.9361	89.8492	R
P5	Coahoma County, MS	34.1542	90.5411	R
P6	Washington County, MS	33.5111	90.8289	S
P7	Sunflower County, MS	33.4031	90.6219	R
P8	Cross County, AR	35.3464	90.4772	R
P9	Phillips County, AR	34.4983	90.6008	R
P10	Azlin Seed Services, OK			S

^aR, resistant; S, sensitive.

420 g ai ha⁻¹ with 1% v/v crop oil concentrate (COC). Herbicide application was made using a research track sprayer equipped with a TTI spray nozzle (TeeJet® spray nozzles, SpraySmarter.com, 455 Merriman Road, Mooresville, IN 46158, USA) calibrated to deliver 140 L ha⁻¹ of herbicide solution at 276 kPa, moving at 2.57 km h⁻¹. Plants were evaluated for visual injury at 21 d after treatment (DAT) on a scale of 0% (no visual injury) to 100% (complete plant mortality). Plant responses to fomesafen were categorized into four groups based on resistance levels: sensitive (>95% control), low resistance (85% to 95% control), moderate resistance (50% to 85% control), and high resistance (<50% control). Data were plotted onto Arkansas and Mississippi state maps in RStudio (v. 3.5.1, RStudio, Boston, MA 02210, USA) using the packages GGplot2, GGmap, and maps.

Genotype–Phenotype Association Analysis on 10 Selected Populations

To further characterize the resistance basis of the *A. palmeri* populations screened, seven representative subsets from the 134 populations, along with three reference populations (two highly PPO inhibitor-resistant populations and one PPO inhibitor-sensitive population) were used for the study (Table 1). Eight plants from these 10 populations at 10 to 15 cm in height were sprayed with fomesafen at the labeled rate of 420 g ai ha⁻¹ with 1% v/v COC, or saflufenacil (Sharpen®, BASF, 26 Davis Drive, P.O. Box 13528, Research Triangle Park, NC 27709, USA) at the labeled rate of 50 g ai ha⁻¹ with 1% v/v methylated seed oil (MSO). Herbicide treatments were applied using a research track sprayer equipped with a TTI spray nozzle as described earlier. Plants were evaluated for visual injury at 21 DAT using the 0% to 100% scale, and visual injury data were then correlated with genotype data from sequencing.

One day before herbicide application, a whole young leaf from the meristem of each individual plant was sampled into 96-well plates (prefilled with metal balls) over dry ice and stored at -80°C until use. Plant tissues were ground in the presence of the Trizol® reagent using a tissue homogenizer and a large paint-shaker. Total RNA was isolated using Direct-zol™ RNA MiniPrep Kits (Zymo Research, 17062 Murphy Avenue, Irvine, CA 92614, USA) following the manufacturer's instructions. Plant RNA was converted to cDNA using a High-Capacity cDNA Reverse Transcription Kit (Applied Biosystems, Thermo Fisher Scientific, 5781 Van Allen Way Carlsbad, CA 92008, USA, cat. no. 4368814) using random primers (20 µl reactions + 200 ng total RNA). The full coding sequence of the *PPX2* gene

(1,580 bp) was amplified using the following primers: AMAPATU.PPX2S-ATG-F; ATGGGCAACATTTCTGAGCGG and AMAPATU.PPX2-TAA-R; TTAYGCGGTCTTCTCATCCATCTTCAC in a 20- μ l PCR reaction that contained: 2 μ l of random primed cDNA template, 0.5 μ M each primer concentration, 10 μ l of Phusion Flash High-Fidelity PCR Master Mix (Thermo Fisher Scientific, cat. no. F-548S), and 16 μ l of nuclease-free H₂O. The thermal cycling condition was 98 C for 10 s; 35 cycles of 98 C for 1 s, 68 C for 5 s, 72 C for 30 s; followed by a final extension for 2 min at 72 C. PCR products were fragmented using the Illumina Nextera XT Library Preparation Kit (Illumina, 5200 Illumina Way, San Diego, CA 92122, USA, cat. no. FC-131-1096) to build a 300-bp cDNA library. The prepared cDNA samples were sequenced using Illumina MiSeq sequencing at the Bayer CropScience facility in Chesterfield, MO. The resulting overlapping sequence reads from all individual R and S plants were assembled into the reference *PPX2* sequence (GenBank accession nos.: DQ386114.1 and MF583744.1). Quality and adaptor trimming were done in CLC Bio Genomics Cloud Engine 1.1.1. Heterozygous and homozygous calls for each single-nucleotide polymorphism were exported from CLC Bio Genomics and used for genotype–phenotype association analysis.

To determine whether *PPX2* overexpression contributes to resistance in these populations, a TaqMan® Gene Expression Assay (Thermo Fisher Scientific) to detect *PPX2* transcript expression level was designed. The sequences for the fluorescent probe, forward and reverse primers, respectively, were: *PPX2_800P*: ACTGACCAATTCCC; *PPX2-800F*: GAGGTGCTGTCCTTGT CATAACA; *PPX2-800R*: CAGCATCATAAGATTGATCTTCAC TGGTA. The translocon of the outer chloroplastic membrane (*Toc75*) was used as one copy reference gene (Shauck 2014). The *Toc75* sequences for the fluorescent probe, forward and reverse primers, respectively, were: *Toc75_3-2 P*: 6FAM-AGC AGCCATATTGC-MGB; *Toc75_3-2 F*: TGTGAAGAGATTAC AACACGGGATG; *Toc75_3-2 R*: TGGCAAAATCCTCTGGC CAGTAG). Each 10- μ l reaction volume contained 5 μ l of TaqMan® Universal 2X Master Mix (Applied Biosystems, Thermo Fisher Scientific, cat. no. 4304437), 1 μ l of 10X TaqMan® Gene Expression Assay, 2.6 μ l of nuclease-free H₂O, 0.2 μ l of each of the 25 μ M forward and reverse primers, and 1 μ l of gDNA or cDNA of all the survivors (~10 ng μ l⁻¹). The TaqMan® assay was conducted using three technical replicates. Relative expression of *PPX2* to *Toc75* was determined using the 2^{- $\Delta\Delta$ Ct} method (Livak and Schmittgen 2001), where Ct is the threshold cycle and Δ Ct is Ct of *Toc75* – Ct of *PPX2*.

Herbicide Dose–Response Studies to Compare the Efficacy of Fomesafen and Saflufenacil

To compare the efficacy of fomesafen and saflufenacil, a more comprehensive herbicide dose–response study was conducted on two highly PPO inhibitor-resistant (R) lines, P1 and P2, and the sensitive (S) line P10. Eight plants from each population at 10 to 15 cm in height were sprayed with fomesafen at 0, 105, 210, 420, 840, 1,680, 3,360, or 6,720 g ai ha⁻¹ with 1% v/v COC or saflufenacil at 0, 6.25, 12.5, 25, 50, 100, 200, or 400 g ai ha⁻¹ with 1% v/v MSO. Herbicide treatments were applied and injury rating was taken as described earlier. Dose–response curves were fit using the four-parameter log-logistic model (Ritz et al. 2016) through the DRC package in RStudio (v. 3.5.1):

$$Y = c + \frac{d - c}{1 + \exp(b(\log(x) - \log(e)))} \quad [1]$$

where *Y* is the visual injury, the upper limit *d* and the lower limit *c* are fixed (e.g., 100 and 0), *b* is the slope, and *e* is the I₅₀ (50% growth inhibition) for each population. The resistant/susceptible (R/S) ratio was calculated by dividing the GR₅₀ (50% growth inhibition) values of the resistant line by that of the sensitive line. Analysis on model fit, parameter estimates, and SE were done through the DRC package in RStudio.

PPX2 Protein Homology Modeling and Computational Docking

All modeling (homology modeling, docking, and ensemble inhibitor–substrate overlap volumes) were calculated using the Molecular Operating Environment (MOE 2018.0101, Chemical Computing Group, Montreal, QC H3A 2R7, Canada). In-house protein sequences for *A. palmeri* *PPX2* were used along with the crystal structure PDB ID: 1SEZ (*Nicotiana tabacum*) template for homology modeling, with a final model minimized using default constraints, and average structure optimized using the AMBER10:EHT force-field and charge model (Cornell et al. 1995). The final protein was subsequently adjusted to the pH 8 charge state using Protonate3D in MOE, and the FAD cofactor was charge corrected to better represent the high-pH milieu of the mitochondria (Labute 2009). All docking was performed using rigid-receptor docking and the GBVI/WSA scoring function (Labute 2008). All mutants were built with direct mutation using the protein builder, except for the Δ Gly-210 deletion, which was built using the homology modeler. All docking poses of each inhibitor or substrate within a 1 kcal mol⁻¹ window were simultaneously loaded as an ensemble, and the intercept volumes between inhibitor–substrate ensemble volumes (ligand–ligand overlap volumes) were calculated using a custom CCG support SVL code, with units in Å³.

Results and Discussion

Spread of Fomesafen Resistance in *Amaranthus palmeri* populations from Arkansas and Mississippi

Plant bioassay results showed that, of the 134 populations screened (90 from Arkansas and 44 from Mississippi), 58% were sensitive to the labeled (1X) rate of fomesafen; 8%, 24%, and 10% of the populations showed low, moderate, and high resistance to fomesafen, respectively (Figure 1). Our resistance frequency is similar to what has been reported in other surveys (Varanasi et al. 2018b). Resistant populations were generally confined to the upper region of the Mississippi River within the two states, close to the borders of the neighboring states Missouri and Tennessee, where widespread occurrence of PPO inhibitor-resistant weeds has been documented (Copeland et al. 2018; Heap 2019; Schultz et al. 2015). Costea et al. (2004) mentioned that *Amaranthus* seeds float easily and can be dispersed by rain, surface irrigation, and watercourses. Therefore, it would be interesting to investigate whether this resistance distribution pattern is partially due to long-distance water dispersal via the Mississippi River or is solely a result of different herbicide usage or agronomic practice history among the sampling sites.

Three Known *PPX2* Mutations Accounted for 90% of the Resistance in the Representative *Amaranthus palmeri* Populations

Analysis of *PPX2* gene expression levels in the plants that survived fomesafen and saflufenacil application at the labeled rate suggests

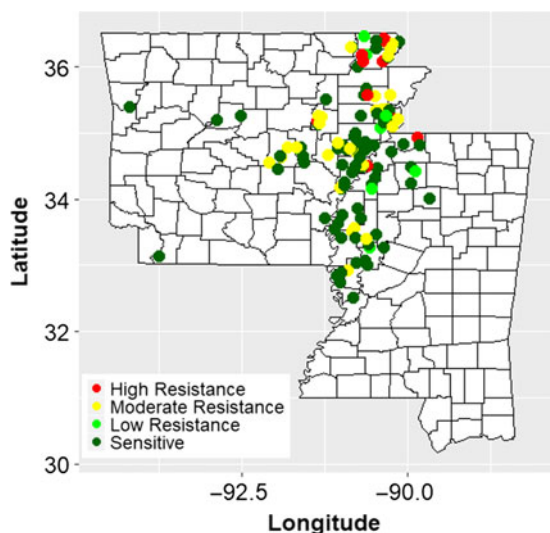


Figure 1. Survey of resistance to fomesafen on 134 *Amaranthus palmeri* populations from Arkansas and Mississippi. Plants were sprayed with fomesafen at 420 g ha⁻¹, and herbicide response was calculated as means of visual control (%) of eight plants from each population, and categorized into four resistance levels: red, high resistance, <50% of control; yellow, moderate resistance, 50%–85% of control; light green, 85%–95% of control, low resistance; and dark green, >95% of control, sensitive.

that the resistance mechanism in these plants was likely not due to increased *PPX2* copy numbers. Similar results were observed in previous studies on resistance to PPO inhibitors in *A. palmeri* surveyed in Arkansas (Salas-Perez et al. 2017; Varanasi et al. 2018b). Genotype–phenotype correlation analysis was conducted only with the three known mutations. We found at least one survivor in 7 out of the 10 populations we sprayed (Table 1). At least one known *PPX2* mutation was present in the seven resistant (R) populations and three known mutations together accounted for resistance in 90% of the survivors (Figure 2).

Among the three mutations, Δ Gly-210 was the most prevalent and was present in four out of seven R populations, followed by Arg-128-Gly and Gly-399-Ala, which were present in three and two populations, respectively. The distribution of the mutations varied among the seven R populations. For three of the seven populations, all the survivors had the same mutation (Δ Gly-210 or Gly-399-Ala) indicating that mutation is likely the most prominent or the sole resistance mechanism in those populations. For two populations, both Arg-128-Gly and Δ Gly-210 mutations were present, in a few cases as double mutations in an individual plant. We did not find any survivors that harbored all three mutations at the same time. There were three populations that had survivors with no known mutations, indicating unknown mutations or a metabolism-based mechanism might be involved, as have been reported in other PPO inhibitor-resistant *Amaranthus* populations (Obenland et al. 2019; Varanasi et al. 2019).

Overall our results suggested that each field might be an independent evolutionary event and that different PPO mutations might be differentially favored during selection. Furthermore, mutations may not account for all resistance to PPO inhibitors. These findings generally agree with previous studies on PPO resistance in *A. palmeri*. In resistant populations collected from Tennessee, Δ Gly-210, and Arg-128-Gly/Met were equally prevalent (~40% frequency), and the two mutations together accounted for 90% of the resistance (Copeland et al. 2018). In resistant populations from Arkansas, Δ Gly-210 (50% frequency) was more prevalent than Arg-128-Gly, and the two mutations were

widespread across and dominated different geographical locations (Salas-Perez et al. 2017; Varanasi et al. 2018b).

While looking at the spread of resistance at the landscape level, the outcrossing nature of *A. palmeri* posts another layer of concern, especially surrounding the coevolution of resistance (Lillie et al. 2019). Many *Amaranthus* species are dioecious, and interspecies hybridization among the *Amaranthus* family is known to facilitate the transfer of herbicide-resistance mechanisms (Franssen et al. 2001; Gaines et al. 2012; Nandula et al. 2014; Trucco et al. 2005). In *A. tuberculatus* var. *rudis*, a species closely related species to *A. palmeri*, Δ Gly-210 was the only known mutation at the target site conferring resistance to PPO inhibitors (Lee et al. 2008; Patzoldt et al. 2006; Thinglum et al. 2011; Wuerffel et al. 2015a). Recently, a novel mutation, Arg-128-Gly/Ile, was reported; and the spreading of resistance-endowing mutations through gene flow between *A. tuberculatus* var. *rudis* and other *Amaranthus* species (e.g., tumble pigweed [*Amaranthus albus* L.] and *A. palmeri*) has been observed (Nie et al. 2019). These studies suggest that controlling weeds before they reproduce will be very critical to restraining the spread of PPO-inhibitor resistance.

Dose–Response Studies on Highly Resistant Populations

The dose–response study on the two highly resistant populations (P1 and P2) showed that saflufenacil was more potent than fomesafen. The I₅₀ values for fomesafen were 28.5 and 12.4 g for the two resistant populations P1 and P2, respectively, and 1.0 g for the susceptible population P10. The I₅₀ values for saflufenacil were 2.4, 2.1, and 0.8 g for P1, P2, and P10, respectively (Figure 3A and B). This is consistent with Salas-Perez et al. (2017), who also observed higher weed efficacy for saflufenacil than fomesafen. The resulting R/S ratios of P1 and P2 were 28 and 12 for fomesafen and 3 and 2.6 for saflufenacil. The higher potency of saflufenacil might be due to its unique physical and chemical properties (e.g., “systemic” attribute, higher dissipation rate) that facilitate the uptake and translocation of the herbicides by weeds (Ashigh and Hall 2010; Mueller et al. 2014).

The spray results for the 10 representative populations also confirmed the higher potency of saflufenacil. Of the 80 plants sprayed for each herbicide, 39% survived fomesafen, while only 8% survived saflufenacil (Figure 4). Furthermore, fomesafen survivors were more robust than saflufenacil survivors, with 18% of the survivors being highly resistant (<50% control). In contrast, saflufenacil had only a few moderate- (50% to 85% control) and low-resistance (85% to 95% control) survivors (Figure 4A and B). The higher potency of saflufenacil might be related to its unique physical/chemical properties that enable phloem mobility and facilitate herbicide translocation within the weeds, which other PPO inhibitors such as fomesafen typically lack (Ashigh and Hall 2010).

When looking at the genetic basis of the survivors for each herbicide (Figure 4C and D), fomesafen selected for diverse mutations: 58%, 5%, and 13% of the fomesafen survivors harbored Δ Gly-210, Arg-128-Gly, and Gly-399-Ala, respectively. Of the survivors, 16% appeared to have none of the known *PPX2* mutations. In contrast, in the 6 saflufenacil survivors out of the 80 sprayed plants, only Δ Gly-210 was found. These results suggest that saflufenacil is likely less sensitive to known *PPX2* mutations. Multiple factors might contribute to different resistance-endowing mutations for fomesafen and saflufenacil. First, saflufenacil has unique phloem mobility (Ashigh and Hall 2010), faster degradation rates (Mueller et al. 2014) and higher potencies, as discussed earlier, which together might subject weeds to different magnitudes and duration of

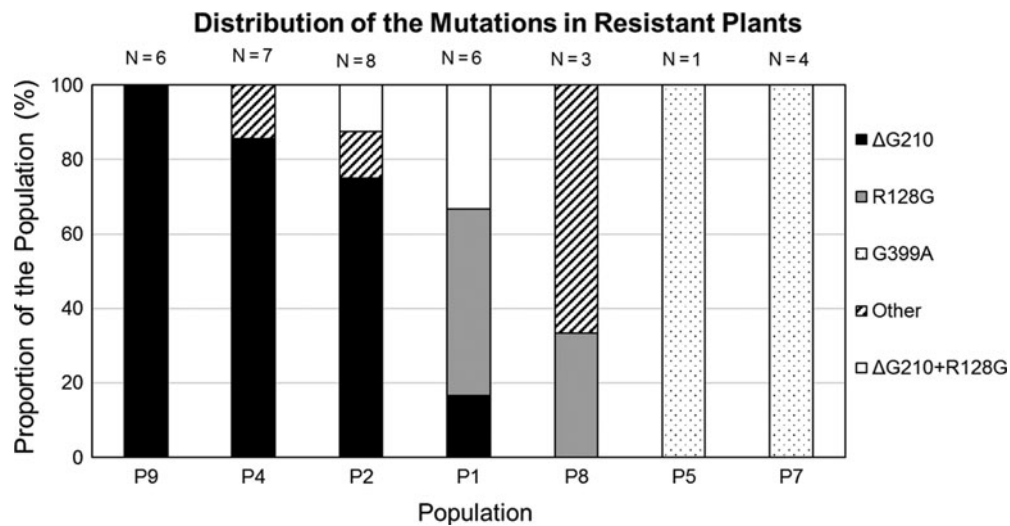


Figure 2. Distribution of different *PPX2* mutations in the survivors across different populations. N is the number of survivors for each population; the solid black bar represents Δ Gly-210; the solid gray bar represents Arg-128-Gly; the dotted white bar represents Gly-399-Ala; the solid white bar represents a double mutation of Δ Gly-210 + Arg-128-Gly; and the dashed bar represents unknown mechanisms.

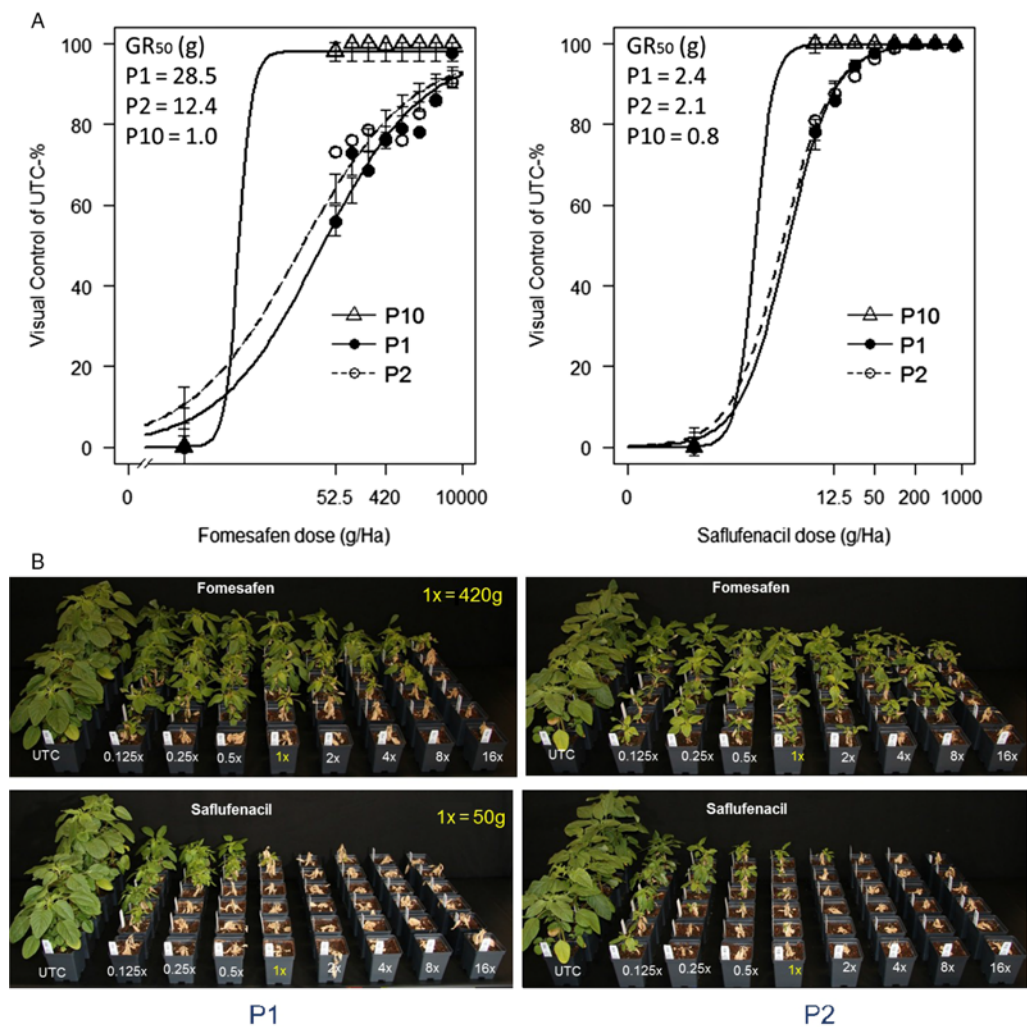


Figure 3. Dose–response studies of fomesafen and saflufenacil on two highly resistant and one susceptible *Amaranthus palmeri* populations. (A) Dose–response curves fit on visual injury of two herbicides on the three *A. palmeri* populations; (B) photos of the dose–response study taken at 21 DAT. UTC, untreated control.

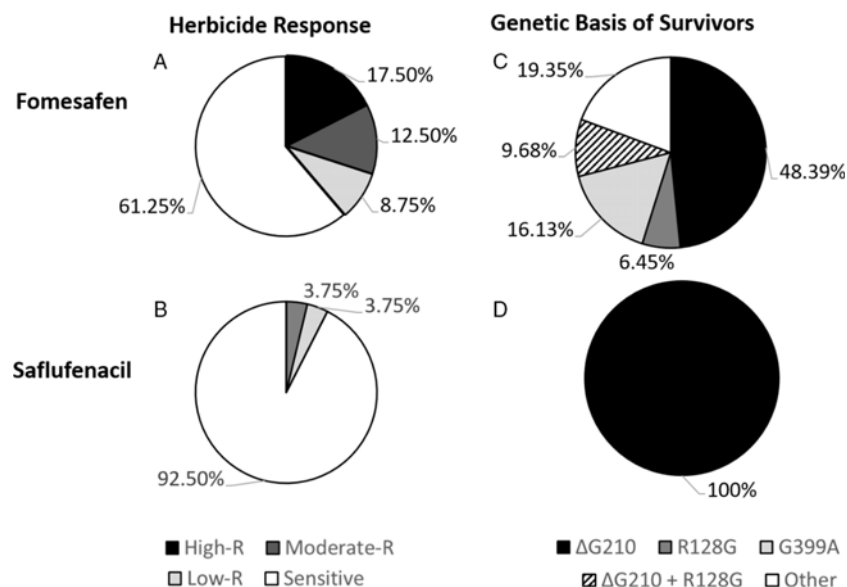


Figure 4. Comparison of herbicide efficacy and resistance genetic basis for the two protoporphyrinogen oxidase (PPO) herbicides. The left panels (A and B) shows distributions of resistance levels in the survivors of each herbicide out of 80 sprayed plants (fomesafen: $N = 31$; saflufenacil: $N = 6$); the right panels (C and D) show the distribution of three *PPX2* mutations among the survivors.

selection pressure. Second, saflufenacil is a relatively newer herbicide, commercially introduced in 2010 (Grossmann et al. 2010); thus, weed populations might have been subjected to a shorter period of selection pressure for saflufenacil than fomesafen.

Differential Binding Affinities and Sensitivities of the Two PPO Inhibitors to the Known *PPX2* Mutations

Our protein/small-molecule modeling was based on the crystal structure of protoporphyrinogen IX oxidase (1SEZ) of *Nicotiana tabacum* (Koch et al. 2004). Our modeling work shows that three known naturally occurring herbicide-resistant mutations all sit at the binding pocket of the herbicide target protein PPO (specifically *PPX2*) and are within a 6.5-Å radius of the docked protoporphyrinogen substrate as shown in ligand-interaction maps (Figure 5). Simple 3D and 2D descriptors for volume and hydrophobic accessible surface area for both inhibitors suggest that the larger the volume of the inhibitor, the greater chance it would be able to fill the active site and competitively inhibit or block the substrate (Table 2, entries 1–3). In addition, changes to the protein binding site microstructure and electrostatics based on *in silico* mutagenesis reduce herbicide binding affinity to different extents. Docking pose scores (a measure of complementarity and surrogate for affinity, in kcal mol⁻¹ using the GBVI/WSA scoring function) for the substrate and two PPO inhibitors studied suggested the binding order was substrate > saflufenacil > fomesafen, in line with experimental findings, although the differential binding affinity is within 1 kcal mol⁻¹ of the substrate, which is within the noise of the method (Table 2, entries 4–7, 12–15). One way of interpreting these binding scores is that although fomesafen binds equivalent to or more weakly than saflufenacil relative to the natural substrate (protoporphyrinogen), certain mutations (such as Arg-128-Gly) pose a significant advantage relative to the natural substrate. Another way of interpreting similar ranges in binding affinity is that it is not only how well an inhibitor binds relative to the substrate in the wild-type and mutant forms, but also how well it physically competes or overlaps with the natural substrate's ability

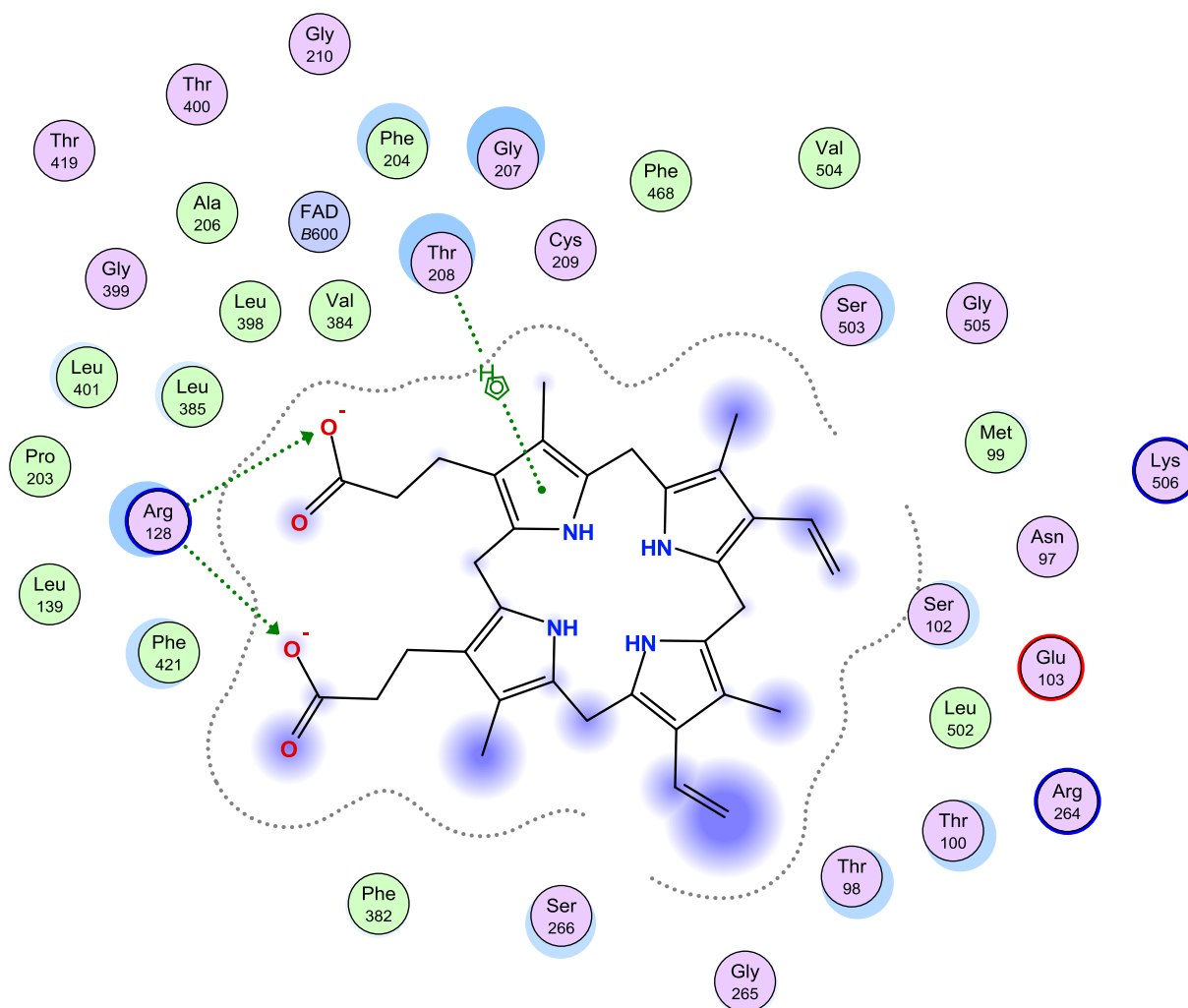
to adopt a catalytically competent geometry; this raises the importance of inhibitor/substrate overlap volume.

One should also note from datum point 14 (Table 2) that the natural substrate binds substantially better to ΔGly-210 than to wild type or other mutations (i.e., approaching 2 kcal mol⁻¹ difference), suggesting another plausible reason for the prevalence of this mutation in the field and a possible energetic basis for a fitness benefit conferred by this mutation or, more accurately, this deletion. However, further pose analysis to understand not only how well the inhibitors bind, but how they compete with the volume of the substrate was quantified by calculating the analytical volume for the pose ensemble. Saflufenacil has greater volume coverage and intercept volume with the substrate than fomesafen (Figure 6; Table 2, entries 8–11) for wild type, ΔGly-210, and Gly-399-Ala, but not for Arg-128-Gly. In the case of the Arg-128-Gly mutation the energy of saflufenacil is still substantially lower than that of fomesafen.

Our protein modeling results suggest that true competitive inhibition, and ultimately efficacy/potency, is a function of both (1) active site binding affinity or how well the inhibitor binds to the active site and (2) better physical “blocking” of the substrate (better inhibitor overlap volume with the substrate). Our results showed that fomesafen had much smaller ensemble volume and overlap volume with the substrate relative to saflufenacil in the “herbicide-resistant” binding pocket, indicating that even minor changes on the protein could be sufficient to confer resistance to the former over the latter. This computational characterization of resistance-forming potential of fomesafen and PPO protein interaction modeling appears to support our genotype–phenotype association analysis, as well as other field surveys showing widespread fomesafen resistance (Salas-Perez et al. 2017; Varanasi et al. 2018b). To reiterate, our protein work also demonstrated that true competitive inhibition will be a function of (1) preferential binding to the pocket while (2) maximally overlapping with the substrate so that catalytically competent substrate poses are no longer accessible. From a herbicide discovery perspective, using these computational strategies to evaluate prospective

Table 2. Protein modeling work on different PPO inhibitors.

	Computed value	Fomesafen	Saflufenacil	Protoporphyrinogen	Units
1	Average of 3D volume	305	354	515	Å ³
2	Average of 2D vdW_vol (van der Waals volume)	403	467	676	Å ³
3	Average of ASA_H (Accessible hydrophobic surface area)	593	631	740	Å ²
4	Score _{inhibitor} - Score _{substrate} : wild-type AMAPA_PPX2	0.2	0.2		kcal/mol
5	Score _{inhibitor} - Score _{substrate} : R128G_AMAPA_PPX2	-0.2	-0.8		kcal/mol
6	Score _{inhibitor} - Score _{substrate} : deltaG210_AMAPA_PPX2	1.7	1.4		kcal/mol
7	Score _{inhibitor} - Score _{substrate} : G399A_AMAPA_PPX2	1.1	0.6		kcal/mol
8	ligand-substrate volume overlap: wild-type AMAPA_PPX2	322	494		Å ³
9	ligand-substrate volume overlap: R128G_AMAPA_PPX2	575	517		Å ³
10	ligand-substrate volume overlap: deltaG210_AMAPA_PPX2 Å ³	373	430		Å ³
11	ligand-substrate volume overlap: G399A_AMAPA_PPX2 Å ³	556	690		Å ³
12	Score _{substrate} : wild-type AMAPA_PPX2			-8.3	kcal/mol
13	Score _{substrate} : R128G_AMAPA_PPX2			-8.1	kcal/mol
14	Score _{substrate} : deltaG210_AMAPA_PPX2			-9.8	kcal/mol
15	Score _{substrate} : G399A_AMAPA_PPX2			-8.4	kcal/mol

**Figure 5.** Ligand interaction diagram of substrate within the active site (6.5 Å). Ligand interaction map of *Amaranthus palmeri* PPO homology model with bound protoporphyrinogen substrate showing all residues within 6.5 Å from the substrate. Other prospective mutants could, in theory, be modeled in silico and tested using the same protocol.

inhibitor/target-site (homology models) interactions should hold promise in a rational agrochemical design strategy to identify better inhibitors with greater resistance-breaking potential. This modeling approach may also hold value in understanding

and prioritizing the resistance-breaking potential of current herbicides for novel target-site mutations yet to be observed in the field, as well as for computationally assisted herbicide-tolerant trait selection.

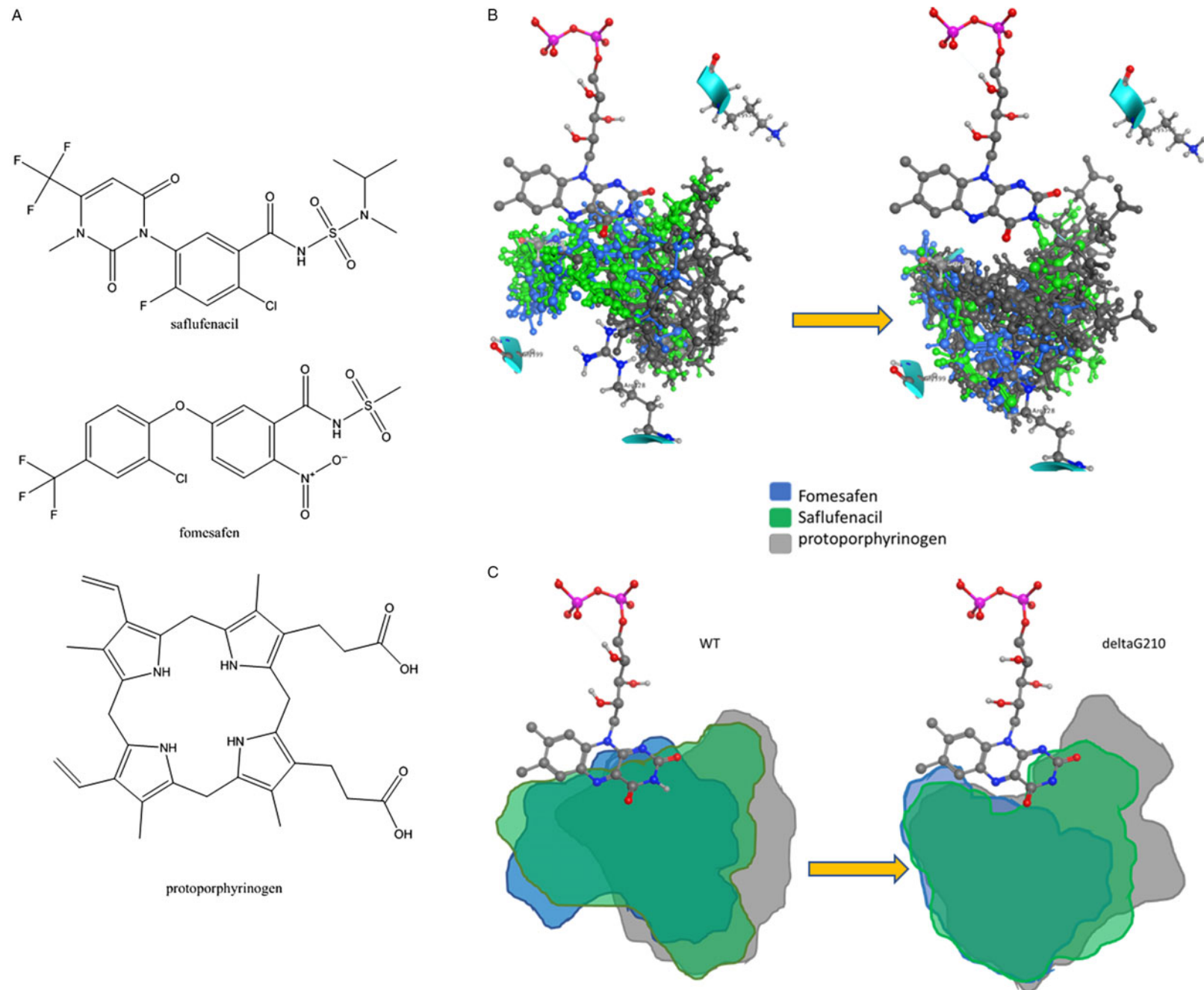


Figure 6. Protein modeling of PPX2 and deletion effects on overlap. (a) Chemical structure of the protoporphyrinogen oxidase (PPO) substrate protoporphyrinogen and two inhibitors; (b) pose analysis to show the competition for the volume with the substrate; (c) volume coverage and intercept volume.

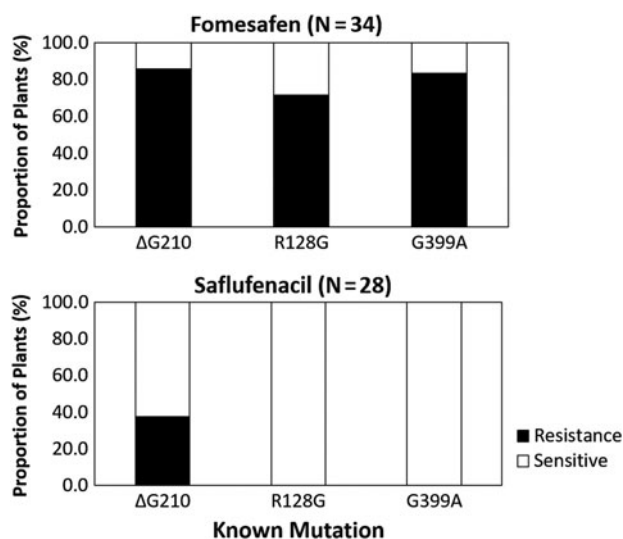


Figure 7. Distribution of three *PPX2* mutations in both resistant and sensitive plants for fomesafen and saflufenacil. N is the total number of all three *PPX2* mutations found among 80 total plants; the black bar represents resistant plants and the white bar represents sensitive plants.

Three Known *PPX2* Mutations Do Not Always Lead to Resistance

To determine whether different mutations are equally effective and sufficient in conferring resistance, we compared the presence of mutations in both resistant and sensitive plants (Figure 7). This type of investigation has not been done very often, as there is generally more interest on the resistance phenotypes. In the 80 plants sprayed with fomesafen, 21, 7, and 6 plants had Δ Gly-210, Arg-128-Gly, and Gly-399-Ala mutations, respectively, 70% to 80% of which were associated with a resistance phenotype. This indicates the three mutations are mostly sufficient to confer resistance to fomesafen. In the 80 plants sprayed with saflufenacil, 16, 8, and 4 plants had Δ Gly-210, Arg-128-Gly, and Gly-399-Ala mutations, respectively. However, only 38% of the plants having Δ Gly-210 turned out to be resistant. None of the plants that harbored Arg-128-Gly or Gly-399-Ala were resistant to saflufenacil (Figure 7).

Our findings were somewhat unexpected, as previous studies indicate that Δ Gly-210, Arg-128-Gly, and Gly-399-Ala can confer similar magnitude(s) of resistance (Dayan et al. 2017; Rangani et al. 2019). The fact that plants with Gly-399-Ala and Arg-128-Gly failed to survive saflufenacil indicates the magnitude of resistance might be population dependent and the roles of different mutations in resistance evolution might be more complex than we thought. Another indication from this observation is that changes to the binding site geometry (volume) and charges (electrostatics) conferred by Arg-128-Gly and Gly-399-Ala mutations might have a difference fitness cost relative to Δ Gly-210 (Dayan et al. 2010) to combat PPO inhibitors with higher potencies like saflufenacil. As a result, weeds might need to evolve a stronger mutation or multiple mechanisms to gain robust resistance. On the other hand, because the efficacy of PPO inhibitors is dependent on plant size (Dayan et al. 2017; Wuerffel et al. 2015a, 2015b) and can be affected by different environmental and physiological conditions (Matzenbacher et al. 2014), it is also possible that bigger plants with known *PPX2* mutations could still survive saflufenacil. Therefore, it is strongly recommended that farmers always spray weeds at smaller sizes to avoid reduced activities and potential risk of resistance development.

Bridging Weed Resistance Knowledge with Management Programs

In this paper, we compared the efficacy and prominent TSR mechanisms for two PPO inhibitors. Our findings showed that, although resistance to some PPO inhibitors such as fomesafen is widespread, certain PPO inhibitors such as saflufenacil are still very effective in killing those resistant weeds. The genetic basis of resistance might vary with different PPO inhibitors and geographic origins. From a weed management perspective, understanding the genetic basis of resistance in a field could potentially allow farmers to switch to other more potent PPO inhibitors that are less affected by the mutations that are present, with the condition that herbicides with different mode of actions are also incorporated.

Furthermore, our protein modeling efforts provide seemingly obvious, yet nontrivial findings that suggest some PPO-inhibitor chemistries can be more sensitive to mutations and protein structure changes than others and that computational modeling approaches could be used to design new chemistries or reprioritize old chemistries for resistance-breaking potential for PPO inhibitors. The current study demonstrated the potential of this valuable tool in the modern agriculture repertoire for providing more robust herbicide/trait combinations to farmers.

Finally, NTSR for PPO inhibitors has been reported and can potentially be reversed by application of metabolism inhibitors (Obenland et al. 2019; Varanasi et al. 2019). Furthermore, NTSR and TSR mechanisms can act together simultaneously, endowing weeds with higher levels of resistance to PPO inhibitors, as has been reported in weeds that are resistant to other herbicide groups (Alcántara-de la Cruz et al. 2017; Fang et al. 2019). Therefore, future research should aim at uncoupling NTSR mechanisms for PPO inhibitors from TSR mechanisms and at elucidating the concerted roles of these two types of resistance mechanisms in a single weed population.

Acknowledgments. The authors would like to thank Brandi Chiapelli for valuable help with total RNA extraction and cDNA preparation for Illumina sequencing; Brian Eads for assistance with upstream sequencing analysis; Jenny Krebel, Megan Gilley, and Jeff Haines for plant propagation and herbicide application; Chris Williams for CCG's SVL support code for ligand-ligand volume overlap and Chandra Aradhya for proofreading the manuscript. No conflicts of interest have been declared.

References

- Alcántara-de la Cruz R, Fernández-Moreno PT, Ozuna CV, Rojano-Delgado AM, Cruz-Hipolito HE, Domínguez-Valenzuela JA, Barro F, De Prado R (2017) Target and non-target site mechanisms developed by glyphosate-resistant hairy beggarticks (*Bidens pilosa* L.). *Front Plant Sci* 7:1492
- Ashigh J, Hall JC (2010) Bases for interactions between saflufenacil and glyphosate in plants. *J Agric and Food Chem* 58:7335–7343
- Beale SI, Weinstein JD (1990) Tetrapyrrole metabolism in photosynthetic organisms. Pages 287–391 in Dailey HA, ed. *Biosynthesis of Heme and Chlorophylls*. New York: McGraw-Hill
- Bi B, Wang Q, Coleman J, McElroy J, Peppers J, Hall N (2019) Single nucleotide polymorphism in plastid protoporphyrinogen oxidase gene (PPO1) confers resistance to oxidiazon in *Eleusine indica*. Abstract 254 in *Proceedings of the 59th Annual Meeting of Weed Science Society of America*. New Orleans, LA: Weed Science Society of America
- Choi KW, Han O, Lee HJ, Yun YC, Moon YH, Kim MK, Kuk YI, Han SU, Guh JO (1998) Generation of resistance to the diphenyl ether herbicide, oxyfluorfen, via expression of the *Bacillus subtilis* protoporphyrinogen oxidase gene in transgenic tobacco plants. *Biosci Biotechnol Biochem* 62:558–560

- Copeland JD, Giacomini DA, Tranel PJ, Montgomery GB, Steckel LE (2018) Distribution of *PPX2* mutations conferring PPO-inhibitor resistance in Palmer amaranth populations of Tennessee. *Weed Technol* 32:592–596
- Cornell WD, Cieplak P, Bayly CI, Gould IR, Merz KM Jr., Ferguson DM, Spellmeyer DC, Fox T, Caldwell JW, Kollman PA (1995) A second generation force field for the simulation of proteins and nucleic acids. *J Am Chem Soc* 117:5179–5197
- Costea M, Weaver SE, Tardif FJ (2004) Biology of Canadian weeds 130. *Amaranthus retroflexus* L., *A. powellii* S. Watson and *A. hybridus* L. *Can J Plant Sci* 84:631–668
- Dayan FE, Barker A, Tranel PJ (2017) Origins and structure of chloroplastic and mitochondrial plant protoporphyrinogen oxidases: implications for the evolution of herbicide resistance. *Pest Manag Sci* 74:2226–2234
- Dayan FE, Daga PR, Duke SO, Lee RM, Tranel PJ, Doerksen RJ (2010) Biochemical and structural consequences of a glycine deletion in the α -8 helix of protoporphyrinogen oxidase. *Biochim Biophys Acta* 1804:1548–1556
- Duke SO, Lydon J, Becerril JM, Sherman TD, Lehnen LP, Matsumoto H (1991) Protoporphyrinogen oxidase-inhibiting herbicides. *Weed Sci* 39:465–473
- Evans CM, Strom SA, Riechers DE, Davis AS, Tranel PJ, Hager AG (2019) Characterization of a waterhemp (*Amaranthus tuberculatus*) population from Illinois resistant to herbicides from five site-of-action groups. *Weed Technol* 33:400–410
- Fang J, Zhang Y, Liu T, Yan B, Li J, Dong L (2019) Target-site and metabolic resistance mechanisms to penoxsulam in barnyardgrass (*Echinochloa crus-galli* (L.) P. Beauv.). *J Agric Food Chem* 67:8085–8095
- Franssen AS, Skinner DZ, Al-Khatib K, Horak MJ, Kulakow PA (2001) Interspecific hybridization and gene flow of ALS resistance in *Amaranthus* species. *Weed Sci* 49:598–606
- Gaines TA, Ward SM, Bukun B, Preston C, Leach JE, Westra P (2012) Interspecific hybridization transfers, a previously unknown glyphosate resistance mechanism in *Amaranthus* species. *Evol Appl* 5:29–38
- Giacomini DA, Umphres AM, Nie H, Mueller TC, Steckel LE, Young BG, Scott RC, Tranel PJ (2017) Two new *PPX2* mutation associated with resistance to PPO inhibiting herbicides in *Amaranthus palmeri*. *Pest Manag Sci* 73:1559–1563
- Grimm B (1998) Novel insights in the control of tetrapyrrole metabolism of higher plants. *Curr Opin Plant Biol* 1:245–250
- Grossmann K, Niggeweg R, Christiansen N, Looser R, Ehrhardt T (2010) The herbicide saflufenacil (Kixor™) is a new inhibitor of protoporphyrinogen IX oxidase activity. *Weed Sci* 58:1–9
- Harder DB, Nelson KA, RJ Smeda (2012) Management options and factors affecting control of a common waterhemp (*Amaranthus rudis*) biotype resistant to protoporphyrinogen oxidase-inhibiting herbicides. *Int J Agron* 2012:1–7
- Heap I (2019) The International Survey of Herbicide Resistant Weeds. <http://www.weedscience.org>. Accessed: November 2, 2019
- Heinemann IU, Jahn M, Jahn D (2008) The biochemistry of heme biosynthesis. *Arch Biochem Biophys* 474:238–251
- Jacobs JM, Jacobs NJ (1993) Porphyrin accumulation and export by isolated barley (*Hordeum vulgare*) plastids. *Plant Physiol* 101:1181–1187
- Koch M, Breithaupt C, Kiefersauer R, Freigang J, Huber R, Messerschmidt A (2004) Crystal structure of protoporphyrinogen IX oxidase: a key enzyme in haem and chlorophyll biosynthesis. *EMBO J* 23:1720–1728
- Labute P (2008) The generalized Born/volume integral implicit solvent model: estimation of the free energy of hydration using London dispersion instead of atomic surface area. *J Comput Chem* 29:1693–1698
- Labute P (2009) Protonate3D: assignment of ionization states and hydrogen coordinates to macromolecular structures. *Proteins* 75:187–205
- Larue CT, Ream JE, Zhou X, Moshiri F, Howe A, Goley M, Sparks OC, Voss ST, Hall E, Ellis C, et al. (2019) Microbial HemG-type protoporphyrinogen IX oxidase enzymes for biotechnology applications in plant herbicide tolerance traits. *Pest Manag Sci* doi:10.1002/ps.5613
- Lee HJ, Duke SO (1994) Protoporphyrinogen IX-oxidizing activities involved in the mode of action of peroxidizing herbicides. *J Agric Food Chem* 42:2610–2618
- Lee HJ, Lee SB, Chung JS, Han SU, Han O, Guh JO, Jeon JS, An G, Back K (2000) Transgenic rice plants expressing a *Bacillus subtilis* protoporphyrinogen oxidase gene are resistant to diphenyl ether herbicide oxyfluorfen. *Plant Cell Physiol* 41:743–749
- Lee R, Hager A, Tranel PJ (2008) Prevalence of a novel resistance mechanism to PPO-inhibiting herbicides in waterhemp (*Amaranthus tuberculatus*). *Weed Sci* 56:371–375
- Lermontova I, Kruse E, Mock HP, Grimm B (1997) Cloning and characterization of a plastidial and a mitochondrial isoform of tobacco protoporphyrinogen IX oxidase. *Proc Natl Acad Sci USA* 94:8895–8900
- Lillie KJ, Giacomini DA, Green JD, Tranel PJ (2019) Coevolution of resistance to PPO inhibitors in waterhemp (*Amaranthus tuberculatus*) and Palmer amaranth (*Amaranthus palmeri*). *Weed Sci* 67:521–526
- Livak KJ, Schmittgen TD (2001) Analysis of relative gene expression data using real-time quantitative PCR and the $2^{-\Delta\Delta C_T}$ method. *Methods* 25:402–408
- Matzenbacher FO, Vidal RA, Merotto JA, Trezzi MM (2014) Environmental and physiological factors that affect the efficacy of herbicides that inhibit the enzyme protoporphyrinogen oxidase: a literature review. *Planta Daninha* 32:457–463
- Mueller, TC, Boswell BW, Mueller SS, Steckel LE (2014) Dissipation of fomesafen, saflufenacil, sulfentrazone, and flumioxazin from a Tennessee soil under field conditions. *Weed Sci* 62:664–671
- Nandula VK, Wright AA, Bond JA, Ray JD, Eubank TW, Molin WT (2014) EPSPS amplification in glyphosate-resistant spiny amaranth (*Amaranthus spinosus*): a case of gene transfer via interspecific hybridization from glyphosate-resistant Palmer amaranth (*Amaranthus palmeri*). *Pest Manag Sci* 70:1902–1909
- Nie HB, Mansfield C, Harre NT, Young JM, Steppig NR, Young BG (2019) Investigating target-site resistance mechanism to the PPO-inhibiting herbicide fomesafen in waterhemp and interspecific hybridization of *Amaranthus* species using next generation sequencing. *Pest Manag Sci* 75:3235–3244
- Obenland OA, Ma R, O'Brien SR, Lygin AV, Riechers DE (2019) Carfentrazone-ethyl resistance in an *Amaranthus tuberculatus* population is not mediated by amino acid alterations in the PPO2 protein. *PLoS ONE* 14:e0215431
- Patzoldt WL, Hager AG, McCormick JS, Tranel PJ (2006) A codon deletion confers resistance to herbicides inhibiting protoporphyrinogen oxidase. *Proc Natl Acad Sci USA* 103:12329–12334
- Rangani G, Salas-Perez RA, Aponte RA, Knapp M, Craig IR, Mietzner T, Langaro AC, Noguera MM, Porri A, Roma-Burgos N (2019) A novel single-site mutation in the catalytic domain of protoporphyrinogen oxidase IX (PPO) confers resistance to PPO-Inhibiting herbicides. *Front Plant Sci* 10:568
- Ritz C, Baty F, Streibig JC, Gerhard D (2016) Dose-response analysis using R. *PLoS ONE* 10:e0146021
- Rousonelos SL, Lee RM, Moreira MS, VanGessel MJ, Tranel PJ (2012) Characterization of a common ragweed (*Ambrosia artemisiifolia*) population resistant to ALS- and PPO-inhibiting herbicides. *Weed Sci* 60:335–344
- Salas-Perez RA, Burgos NR, Rangani G, Singh S, Refatti JP, Pivetam L, Tranel PJ, Mauromoustakos A, Scott RC (2017) Frequency of Gly-210 deletion mutation among protoporphyrinogen oxidase inhibitor-resistant Palmer amaranth (*Amaranthus palmeri*) populations. *Weed Sci* 65:718–731
- Schultz JL, Chatham LA, Riggins CW, Tranel PJ, Bradley KW (2015) Distribution of herbicide resistances and molecular mechanisms conferring resistance in Missouri waterhemp (*Amaranthus rudis* Sauer) populations. *Weed Sci* 63:336–345
- Selby TP, Ruggiero M, Hong W, Travis DA, Satterfield AD, Ding AX (2015) Broad-spectrum PPO-inhibiting N-phenoxyphenyluracil acetal ester herbicides. *ACS Symp Ser* 1204:277–289
- Shauck TC (2014) Identification of Nontarget-Site Mechanisms of Glyphosate Resistance in Roots and Pollen of *Amaranthus* and *Ambrosia*. Ph.D dissertation. Columbia: University of Missouri. 92 p
- Shergill LS, Barlow BR, Bish MD, Bradley KW (2018) Investigations of 2,4-D and multiple herbicide resistance in a Missouri waterhemp (*Amaranthus tuberculatus*) population. *Weed Sci* 66:386–394
- Thinglum KA, Riggins CW, Davis AS, Bradley KW, Al-Khatib K, Tranel PJ (2011) Wide distribution of the waterhemp (*Amaranthus tuberculatus*) Δ G210 *PPX2* mutation, which confers resistance to PPO-inhibiting herbicides. *Weed Sci* 59:22–27

- Trucco F, Jeschke MR, Rayburn AL, Tranel PJ (2005) *Amaranthus hybridus* can be pollinated frequently by *A. tuberculatus* under field conditions. *Heredity* 94:64–70
- Varanasi VK, Brabham C, Norsworthy JK (2018a) Confirmation and characterization of non-target site resistance to fomesafen in Palmer amaranth (*Amaranthus palmeri*). *Weed Sci* 66:702–709
- Varanasi VK, Brabham C, Norsworthy JK, Nie H, Young BG, Houston M, Barber T, Scott RC (2018b) A statewide survey of PPO-inhibitor resistance and the prevalent target-site mechanisms in Palmer amaranth (*Amaranthus palmeri*) accessions from Arkansas. *Weed Sci* 66:149–158
- Varanasi VK, Brabham C, Korres NE, Norsworthy JK (2019) Nontarget site resistance in Palmer amaranth [*Amaranthus palmeri* (S.) Wats.] confers cross-resistance to protoporphyrinogen oxidase-inhibiting herbicides. *Weed Technol* 33:349–354
- von Wettstein D, Gough S, Kannangara CG (1995) Chlorophyll biosynthesis. *Plant Cell* 7:1039–1057
- Watanabe N, Che FS, Iwano M, Takayama S, Yoshida S, Isogai A (2001) Dual targeting of spinach protoporphyrinogen oxidase II to mitochondria and chloroplasts by alternative use of two in-frame initiation codons. *J Biol Chem* 276:20474–20481
- Watanabe N, Takayama S, Yoshida S, Isogai A, Che FS (2002) Resistance to protoporphyrinogen oxidase-inhibiting compound S23142 from overproduction of mitochondrial protoporphyrinogen oxidase by gene amplification in photomixotrophic tobacco cells. *Biosci Biotechnol Biochem* 66:1799–1805
- Wuerffel RJ, Young JM, Lee RM, Tranel PJ, Lightfoot DA, Young BG (2015a) Distribution of the Δ G210 protoporphyrinogen oxidase mutation in Illinois waterhemp (*Amaranthus tuberculatus*) and an improved molecular method for detection. *Weed Sci* 63:839–845
- Wuerffel RJ, Young JM, Matthews JL, Young BG (2015b) Characterization of PPO-inhibitor-resistant waterhemp (*Amaranthus tuberculatus*) response to soil-applied PPO-inhibiting herbicides. *Weed Sci* 63:511–521